The conformal alpha shape filtration

Visual Comput (2006) 22: 531–540
DOI 10.1007/s00371-006-0027-1

ORIGINAL ARTICLE

Frederic Cazals
Joachim Giesen
Mark Pauly
Afra Zomorodian

The conformal alpha shape filtration*

Published online: 24 June 2006

J. Giesen (✉) · M. Pauly
Department of Computer Science, ETH Zurich, Switzerland
{giesen,pauly}@inf.ethz.ch

F. Cazals
INRIA Sophia Antipolis, France
Frederic.Cazals@sophia.inria.fr

A. Zomorodian
Department of Computer Science, Stanford University, USA
afra@cs.stanford.edu

Abstract *Conformal alpha shapes* are a new filtration of the Delaunay triangulation of a finite set of points in $\mathbb{R}^d$. In contrast to (ordinary) alpha shapes the new filtration is parameterized by a local scale parameter instead of the global scale parameter in alpha shapes. The local scale parameter *conforms* to the local geometry and is motivated from applications and previous algorithms in surface reconstruction. We show how conformal alpha shapes can be used for surface reconstruction of non-uniformly sampled surfaces, which is not possible with alpha shapes.

Keywords Alpha shapes · Computational topology · Computational geometry · Surface reconstruction

1 Introduction

The method of *alpha shapes* was originally motivated for the study of points in the plane [9]. This method was later generalized to higher dimensional points [10]. Alpha shapes define a family of simplicial complexes parameterized by $\alpha \in \mathbb{R}$. These *α-complexes* have vertices in the point set and simplices from the points' Delaunay triangulation. Consequently, alpha complexes are efficiently computable. Later the definition of alpha shapes was modified slightly and extended also to weighted points [5]. With the modified definition, the family of alpha shapes implies a *filtration*, a partial ordering of the simplices of the Delaunay triangulation, that may be used for multi-scale topological analysis of the point cloud. It is this rich structure that makes alpha shapes popular in many applications ranging from bio-geometric modeling [8], where atoms are modeled as weighted points, to surface reconstruction, where the surface of some solid is sampled.

Alpha shapes have influenced the development of provable surface reconstruction algorithms in computational geometry. By "provable", we mean geometric and topological guarantees that are based on assumptions on the sampling. We distinguish two major lines of Delaunay-based surface reconstruction algorithms. The first line considers *filtering* the Delaunay triangulation of a point cloud. Alpha shapes is one such filter as each α-complex specifies a subset of the simplices. Beginning with the seminal work of Amenta and Bern, there have been proposed a flurry of such algorithms, the most significant of which are the *Crust* and the *Cocone* algorithms [1, 2]. The second line of research takes the fundamentally differ-

*This research was partially supported by the Swiss National Science Foundation under the project "Non-linear manifold learning" and by DARPA under grant 32905.

ent approach of examining the critical points of a discrete or continuous flow based on the sample points [7, 11]. These critical points are related to the critical α-complex simplices: the simplices at which the complex undergoes a topological change.

Although alpha shapes have inspired fruitful research on surface reconstruction, the method's utility is limited. First, alpha shapes define a family of complexes, but it is not clear which α-complex is suitable for reconstruction. Second, the chosen α fixes a global scale, so the method can be successful only for uniform sampling. The algorithms that have been successful in practice all use local filters to cope with non-uniform sampling.

In this paper, we discuss *conformal alpha shapes*, which use a local scale parameter $\hat{\alpha}$ instead of the global scale parameter α. We show that conformal alpha shapes share many properties with ordinary alpha shapes, but have additional properties that are useful for surface reconstruction. In the rest of the paper, we study the geometric and topological consequences of localizing the scale parameter within the framework of surface reconstruction. We begin by defining conformal alpha shapes in Sect. 2. In Sect. 3 we consider topological repercussions when moving from global to a conformal scale as done with conformal alpha shapes. In Sect. 4, we discuss how conformal alpha shapes can be utilized for surface reconstruction. We prove that conformal alpha shapes at a well defined scale are essentially equivalent to the *Crust* and *Cocone* surface reconstruction algorithms. Finally, we demonstrate the difference between ordinary and conformal alpha shapes with some example that we obtained from our implementation of the conformal alpha shape filtration.

A preliminary version of this paper appeared in [3].

2 Definitions

In this section, we begin by briefly describing the background necessary for our work, including the definition of alpha complexes as a family of sub-complexes of the Delaunay triangulation. We then introduce conformal alpha shapes and prove that they also provide a family of subcomplexes as the prior method.

2.1 Preliminaries

A point set $P \subset \mathbb{R}^d$ is in *general position*, if there are no $k \leq d+1$ points on a common $(k-2)$-flat or $k \leq d+2$ points on a common $(k-3)$-sphere. In the following, we always assume the general position as this assumption simplifies the exposition and is justified in practice [6]. A *k-simplex* σ is the convex hull of $k+1$ points $S \subseteq P$. A simplex τ defined by $T \subseteq S$ is a *face* of σ and σ is a *co-face* of τ. A *simplicial complex* K is a finite set of simplices that meet along faces, all of which are in K. A *filtration* of a complex K is a nested subsequence of complexes $\emptyset = K^0 \subseteq K^1 \subseteq \ldots \subseteq K^m = K$.

The *Voronoï diagram* $V(P)$ of P is a cell decomposition of $\mathbb{R}^d$ into convex polyhedra. Every *Voronoï cell* V_p corresponds to exactly one sample point $p \in P$ and contains all points of $\mathbb{R}^d$ closest to p. That is,

$$V_p = \{x \in \mathbb{R}^d \mid \|x-p\| \leq \|x-q\|, \forall q \in P\}.$$

Closed facets shared by $d-k+1$ Voronoï cells are called *Voronoï k-facets*.

The *Delaunay triangulation* $D(P)$ of P is the dual of the Voronoï diagram. Whenever a collection $V_{p_1}, \ldots, V_{p_k}$ of Voronoï cells have a non-empty intersection, the simplex defined on the corresponding points $p_1, \ldots, p_k$ is in $D(P)$. The Delaunay triangulation is a simplicial complex that decomposes the convex hull of the points in P. In the rest of the paper, all simplices will be Delaunay. At times, we will restate this to remind the reader.

2.2 Alpha shapes

For a given value of $\alpha \in [0, \infty)$, *alpha balls* are balls of radius α around the points in P. The corresponding *alpha complex* of P is the Delaunay triangulation of P restricted to the alpha balls. A simplex belongs to the alpha complex, if the Voronoï cells of its vertices have a common non-empty intersection with the set of alpha balls. Note that at $\alpha = 0$, the alpha complex consists just of the set P, and for sufficiently large α, the alpha complex is the Delaunay triangulation $D(P)$ of P. For any simplex $\sigma \in D(P)$, let $\alpha(\sigma)$ be the α value at which σ appears for the first time in the alpha complex. The alpha shape filtration is the sequence of alpha complexes obtained from growing α from zero to infinity. We show a few complexes from the alpha shape filtration for a small set of points in Fig. 6.

2.3 Conformal alpha shapes

For $p \in P$, let $D_p \subseteq D(P)$ denote the simplices incident on p. The alpha values determine a partial ordering on D_p, one which we make into a total ordering by sorting according to dimension and breaking the remaining ties arbitrarily. We may then view D_p as a sequence of simplices with non-decreasing alpha values $\alpha_p^1 \leq \cdots \leq \alpha_p^n$. Note that $\alpha_p^1 = 0$ since the first simplex in D_p is the point p which appears at $\alpha = 0$. Let $\alpha_p^- < \alpha_p^+$ be two α values in $\{\alpha_p^i\}_i$. We will specify how to choose these values later in the paper. We now re-scale α_p^i using these local values:

$$\hat{\alpha}_p^i = \frac{\alpha_p^i - \alpha_p^-}{\alpha_p^+}.$$

We call $\hat{\alpha}_p^i$ the *internal alpha scale*. This scale is invariant to Euclidean transformations and scaling, so it is *conformal*.

As in alpha shapes, we consider a restricted Delaunay triangulation for each value $\hat{\alpha} \in (-\infty, \infty)$. However, the restriction is not to the set of alpha balls, but to a new set of balls whose radii are determined from their internal alpha scales. We put a ball of radius α_p at each point $p \in P$, where

$$\alpha_p(\hat{\alpha}) = \alpha_p^+ \hat{\alpha} + \alpha_p^-,$$

and a ball of negative radius is defined to be empty. Let $C_p^{\hat{\alpha}}$ be the intersection of the Voronoï cell V_p and the ball at p and let $C^{\hat{\alpha}}$ be the interior of $\cup_{p \in P} C_p^{\hat{\alpha}}$. The *conformal alpha shape (complex)* is the Delaunay triangulation of P restricted to $C^{\hat{\alpha}}$.

As in the definition of $\alpha(\sigma)$, let $\hat{\alpha}(\sigma)$ be the $\hat{\alpha}$ value at which σ appears for the first time in the conformal alpha shape. We may compute the $\hat{\alpha}(\sigma)$ from the value of $\alpha(\sigma)$. Let $p_1, \ldots, p_k \in P$ be the vertices of σ. Then,

$$\hat{\alpha}(\sigma) = \max_{1 \le i \le k} \inf\{\hat{\alpha} \mid \alpha_{p_i}(\hat{\alpha}) \ge \alpha(\sigma)\}. \tag{1}$$

Lemma 1. *The sequence of conformal alpha shapes obtained by growing $\hat{\alpha}$ from zero to infinity is a filtration of the Delaunay triangulation $D(P)$ of P.*

Proof. We need to show the following: (1) If $\hat{\alpha} < \hat{\alpha}'$, the simplices in the conformal $\hat{\alpha}$-shape are also in the conformal $\hat{\alpha}'$-shape. (2) For sufficiently large $\hat{\alpha}$, the conformal $\hat{\alpha}$-shape is $D(P)$. (3) A simplex $\sigma \in D(P)$ is earlier than all its co-faces τ in the filtration, that is, $\hat{\alpha}(\sigma) \le \hat{\alpha}(\tau)$.

Property (1) holds as $C^{\hat{\alpha}} \subset C^{\hat{\alpha}'}$ for $\hat{\alpha} < \hat{\alpha}'$. Property (2) holds as $C^{\hat{\alpha}}$ covers $\mathbb{R}^d$ in the limit as $\hat{\alpha}$ approaches infinity. For property (3), let $S = \{p_i\}_i$ be the vertices of σ. The coface τ also has S as vertices, along with some additional vertices. There exists a point $p_i \in S$ such that

$$\alpha_{p_i}\big(\hat{\alpha}(\sigma)\big) = \alpha(\sigma) \le \alpha(\tau) \le \alpha_{p_i}(\hat{\alpha}(\tau)),$$

which implies $\hat{\alpha}(\sigma) \le \hat{\alpha}(\tau)$ as α_{p_i} is a monotonically increasing function.

3 Topology

In this section, we study both the ordinary and the conformal alpha shape filtrations. A filtration allows us to track topological changes at different scales. Here, the scale parameter is either α or $\hat{\alpha}$. The topology of the respective alpha shapes changes only at a finite number of critical α values as both have a finite number of simplices. We characterize these values and uncover the relationship between the critical values of conformal alpha shapes and those of the ordinary alpha shapes.

A simplex σ is *α-late*, if $\alpha(\rho) < \alpha(\sigma)$ for all faces ρ, and *α-early*, if $\alpha(\sigma) < \alpha(\tau)$ for all co-faces τ. If σ is both α-late and α-early, it is *α-critical*. We similarly have *$\hat{\alpha}$-late*, *$\hat{\alpha}$-early*, and *$\hat{\alpha}$-critical*. We define every vertex to be α- and $\hat{\alpha}$-late and every d-dimensional simplex to be α- and $\hat{\alpha}$-early. Note that by the filtration property we always have $\alpha(\rho) \le \alpha(\sigma) \le \alpha(\tau)$ and $\hat{\alpha}(\rho) \le \hat{\alpha}(\sigma) \le \hat{\alpha}(\tau)$ for faces ρ and co-faces τ of simplex σ.

The α-critical simplices have a simple characterization.

Lemma 2 ([7, 11])**.** *The α-critical Delaunay simplices are exactly those that have a non-empty intersection with their dual Voronoï cells. This intersection is a unique point, namely the center of the smallest enclosing ball of the simplex.*

A similar characterization does not exist for $\hat{\alpha}$-critical simplices but the following is true for both filtrations.

Lemma 3. *The homotopy type of the alpha shape (ordinary or conformal) of a finite point set in general position changes only when a critical simplex enters the shape.*

Proof. Clearly, the homotopy type of an alpha shape (ordinary or conformal) changes when a critical simplex appears. If a k-dimensional critical simplex appears, either the $(k-1)$-th Betti number of the alpha shape decreases by 1, or the kth Betti number increases by 1 in simplicial homology. At the appearance of 0-dimensional simplices (vertices), the 0-th Betti number always increases, and at the appearance of critical d-dimensional simplices, the $(d-1)$-th Betti number always decreases.

In the following, we restrict our exposition to $\hat{\alpha}(\cdot)$, but all arguments also hold for $\alpha(\cdot)$. We need to show that the homotopy type of the alpha shape does not change for non-critical simplices. If a k-dimensional simplex σ is non-critical, then either σ has a $(k-1)$-dimensional face ρ with $\hat{\alpha}(\rho) = \hat{\alpha}(\sigma)$ or σ is the face of a $(k+1)$-dimensional simplex with $\hat{\alpha}(\sigma) = \hat{\alpha}(\tau)$. Note that if $\hat{\alpha}(\rho) = \hat{\alpha}(\sigma)$, then ρ is non-critical and if $\hat{\alpha}(\sigma) = \hat{\alpha}(\tau)$, then τ is non-critical.

Let σ be the highest dimensional simplex involved in a non-critical alpha event, that is, the highest-dimensional simplex among those that appear at the same $\hat{\alpha}$ value. The dimension k of σ is at least two as a non-critical event may not involve just vertices and edges: if an edge is early, it has to be critical as by definition it is always late. By our assumption, σ cannot be early, so it must have at least one $(k-1)$-dimensional face ρ with $\hat{\alpha}(\rho) = \hat{\alpha}(\sigma)$. If we can show that there is exactly one such face ρ, then we are done as there is a straightforward deformation retraction of σ to $\partial\sigma \setminus \rho$ and the homotopy type of the alpha shape does not change.

We need to show that there is only one $(k-1)$-dimensional face ρ of σ with $\hat{\alpha}(\rho) = \hat{\alpha}(\sigma)$. Let $p_1, \ldots, p_{k+1} \in P$ be the vertices of σ. The $(k-1)$-dimensional faces ρ_i of σ are the convex hull of the vertex sets $\{p_1, \dots, p_{k+1}\} \setminus \{p_i\}$ for $1 \le i \le k$. Let V be the Voronoï facet dual to σ and V_i be the Voronoï facet dual to ρ_i. As σ is not $\hat{\alpha}$-late, there is a V_i with

$$\min\{\hat{\alpha} \mid C^{\hat{\alpha}} \cap V_i \neq \emptyset\} = \min\{\hat{\alpha} \mid C^{\hat{\alpha}} \cap V \neq \emptyset\},$$

as $\hat{\alpha}(\rho_i) = \hat{\alpha}(\sigma)$. Now assume that there is another face $\rho_j \neq \rho_i$ with the same property

$$\min\{\hat{\alpha} \mid C^{\hat{\alpha}} \cap V_j \neq \emptyset\} = \min\{\hat{\alpha} \mid C^{\hat{\alpha}} \cap V \neq \emptyset\}.$$

Then, we have

$$C^{\hat{\alpha}(\sigma)} \cap V_i = C^{\hat{\alpha}(\sigma)} \cap V_j = C^{\hat{\alpha}(\sigma)} \cap V.$$

The intersection $C^{\hat{\alpha}(\sigma)} \cap V$ must be a single point since $\hat{\alpha}(\sigma)$ is the smallest $\hat{\alpha}$ such that $C^{\hat{\alpha}} \cap V \neq \emptyset$. Let x be the intersection point. Since $\hat{\alpha}(\rho_i) = \hat{\alpha}(\sigma)$, there must exist a vertex $q \in \rho_i$ with $\operatorname{argmin}_{y \in V_i} \|q - y\| = x$. But any point $y \in V_i$ has the same distance to all vertices of ρ_i. So, for all vertices $q \in \rho_i$,

$$\operatorname*{argmin}_{y \in V_i} \|q - y\| = x.$$

Similarly, for all vertices $r \in \rho_j$,

$$\operatorname*{argmin}_{y \in V_j} \|r - y\| = x.$$

Since σ is at least two-dimensional, i.e., $k \ge 2$, ρ_i and ρ_j must have at least one vertex $p \in P$ in common. For this vertex p,

$$\operatorname*{argmin}_{y \in V_i} \|p - y\| = \operatorname*{argmin}_{y \in V_j} \|p - y\| = x,$$

and x is the center of the circumcircle of the triangle $p_i p_j p$:

$$\|p_i - x\| = \|p_j - x\| = \|p - x\|.$$

By construction, the line through p and p_j is orthogonal to the affine hull of V_i as the line segment pp_j is an edge of ρ_i. Similarly, the line through p and p_i is orthogonal to the affine hull of V_j. But this is impossible since the Voronoï cell V_p is convex and we assumed the point set P is in general position, as shown in Fig. 1.

Therefore $p_i = p_j$, arriving at a contradiction. This completes the proof.

The following lemma implies that we get two permutations of the α-critical simplices according to the α and $\hat{\alpha}$ values, respectively. The difference of these permutations is a measure for the non-uniformity present in the point set P.

Lemma 4. *Every α-critical Delaunay simplex σ is also $\hat{\alpha}$-critical.*

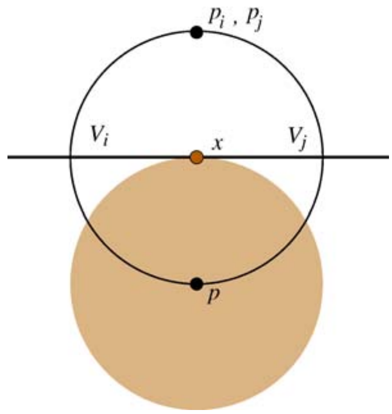

Fig. 1. The only position of p_i and p_j is degenerate, taking the convexity of V_p into account

Proof. Let $p_1, \dots, p_k \in P$ be the vertices of σ. We begin by showing that if σ is α-late, then it is also $\hat{\alpha}$-late. If σ is α-late, $\alpha(\rho_i) < \alpha(\sigma)$ for all its $(k-2)$-dimensional faces ρ_i, $1 \le i \le k$. So,

$$\begin{aligned}
\hat{\alpha}(\rho_i) &= \max_{\substack{1 \le j \le k \\ j \neq i}} \inf\{\hat{\alpha} \mid \alpha_{p_j}(\hat{\alpha}) \ge \alpha(\rho_j)\} \\
&< \max_{\substack{1 \le j \le k \\ j \neq i}} \inf\{\hat{\alpha} \mid \alpha_{p_j}(\hat{\alpha}) \ge \alpha(\sigma)\} \\
&\le \max_{1 \le j \le k} \inf\{\hat{\alpha} \mid \alpha_{p_j}(\hat{\alpha}) \ge \alpha(\sigma)\} \\
&= \hat{\alpha}(\sigma),
\end{aligned}$$

for $1 \le i \le k$. That is, σ is also $\hat{\alpha}$-late. We now show the reverse statement: if σ is α-early, then it is also $\hat{\alpha}$-early. Let τ be any k-dimensional co-face of σ and let p_{k+1} be be the additional vertex of τ. Since σ is α-early, $\alpha(\sigma) < \alpha(\tau)$. We have

$$\begin{aligned}
\hat{\alpha}(\sigma) &= \max_{1 \le j \le k} \inf\{\hat{\alpha} \mid \alpha_{p_j}(\hat{\alpha}) \ge \alpha(\sigma)\} \\
&< \max_{1 \le j \le k} \inf\{\hat{\alpha} \mid \alpha_{p_j}(\hat{\alpha}) \ge \alpha(\tau)\} \\
&\le \max_{1 \le j \le k+1} \inf\{\hat{\alpha} \mid \alpha_{p_j}(\hat{\alpha}) \ge \alpha(\tau)\} \\
&= \hat{\alpha}(\tau).
\end{aligned}$$

Therefore, σ is also $\hat{\alpha}$-early. Since it was $\hat{\alpha}$-late from before, σ is $\hat{\alpha}$-critical.

Note that the reverse of Lemma 4 is not true in general. There can be more $\hat{\alpha}$-critical simplices then there are α-critical ones, as demonstrated in Fig. 2.

4 Surface reconstruction

We wish to use conformal alpha shapes to reconstruct a smooth surface S in $\mathbb{R}^3$ from a finite sampling P. In this section, we describe a geometrical approach very much in line with the philosophy behind the Crust and Cocone

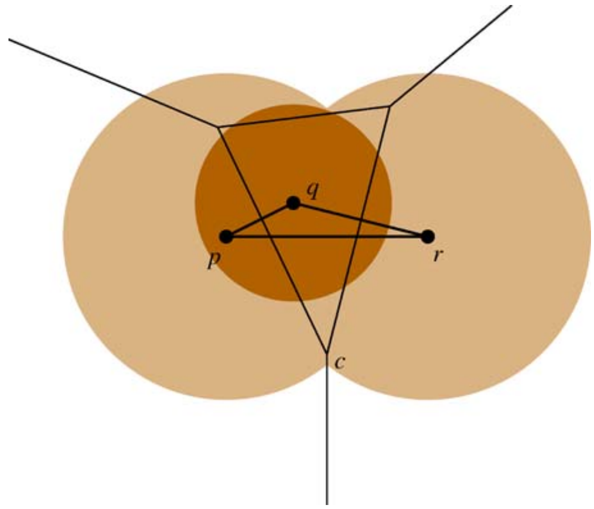

Fig. 2. The reverse of Lemma 4 is not always true. Triangle pqr is $\hat{\alpha}$-critical but not α-critical, if we assume that the poles p^* and r^* are somewhere below (not shown in the figure) and the pole q^* is the circumcenter c of the triangle pqr

algorithms. We begin with the common geometric definitions and then examine the geometry of the reconstruction.

4.1 Preliminaries

Suppose we are given a smooth surface S embedded in $\mathbb{R}^3$. An open ball is *empty*, if it does not contain any point from S. An empty ball is *maximal*, if it is not contained in a larger empty ball. The *medial axis* $M(S)$ of S is the union of the centers of all maximal open balls. The distance of a point $x \in S$ to the medial axis $M(S)$ is its *local feature size*. We define $f: S \to \mathbb{R}$,

$$f(x) = \inf_{y \in M(S)} \|x - y\|,$$

to be the function that assigns the local feature size to a point.

An *ε-sample* of S is a subset $P \subseteq S$ such that every point $x \in S$ has a point $p \in P$ at distance at most $\varepsilon f(x)$. An ϵ-sampling is *uniform*, if every point has a point in P at distance at most $\inf_{x \in S} f(x)$. Although the sampling density may vary non-uniformly across S, the density is bounded below by the smallest feature size. For sufficiently small ε, every ε-sample is uniform but it depends on S what sufficiently small means.

Let V_p be the Voronoï cell of a sample point $p \in P$. If V_p is bounded, we let $\vec{u}$ be the vector from p to the Voronoï vertex in V_p that has the largest distance to p. Otherwise, V_p is unbounded and we let $\vec{u}$ be a vector in the average direction of all unbounded Voronoï edges incident to V_p. The *second pole* of V_p is the Voronoï vertex p^* in V_p with the largest distance to p such that the vector $\vec{u}$ and the vector from p to p^* make an angle larger than $\pi/2$ [1]. For brevity we want to refer to the second pole in the following simply as pole.

4.2 Theoretical guarantees

We begin by specifying the internal alpha scale parameters α_p^- and α_p^+ for a sample point $p \in P$. Let $\alpha_p^- = \alpha_p^1 = 0$. Let α_p^+ be the α value at which the simplex dual to the pole p^* appears in the ordinary alpha shape, that is, $\alpha_p^+ = \|p - p^*\|$. Note that with these values for the parameters, the points in P all appear at $\hat{\alpha} = 0$. This implies that all the simplices appear at non-negative $\hat{\alpha}$ values.

The *restricted Voronoï diagram* $V_S(P)$ is the Voronoï diagram $V(P)$ intersected with the surface S. The *restricted Delaunay triangulation* $D_S(P)$ is its dual and is necessarily a subset of the Delaunay triangulation. In the rest of the section, we use $\eta = \varepsilon/(1-\varepsilon)$ for notational brevity. We begin with the following result.

Lemma 5. *Let P be an ε-sample of a smooth surface S. Then, all conformal alpha shapes for $\hat{\alpha} \geq \eta$ contain $D_S(P)$.*

Proof. For $p \in P$, let α_p^i be the largest α value at which a simplex from $D_S(P)$ incident to p appears in the ordinary alpha shape. By Lemma 6 we have that

$$\alpha_p^i \leq \eta f(p).$$

We also have $\alpha_p^+ \geq f(p)$ by our choice of α_p^+. Therefore,

$$\hat{\alpha}_p^i = \frac{\alpha_p^i}{\alpha_p^+} \leq \frac{\eta f(p)}{\alpha_p^+} \leq \eta.$$

This implies the statement of the lemma.

Essentially, Lemma 5 asserts that the alpha shape for a large enough $\hat{\alpha}$ contains certain simplices, i.e., the restricted ones, of the Delaunay triangulation of a surface sampling. In the following we want to show that the conformal alpha shape does not contain certain simplices, namely, simplices that are too large. For the proof we need an auxiliary lemma.

Lemma 6. *Let P be an ε-sample of a smooth surface S and let $p \in P$ be a sample point. Then,*

(1) For any point x in the cell V_p in $V_S(P)$, $\|p - x\| \leq \eta f(p)$.
(2) For any point x in the intersection of V_p with the hyperplane containing p and orthogonal to $p^* - p$,

$$\|x - p\| \leq \frac{\eta f(p)}{\sin\left(\frac{\pi}{2} - 3 \arcsin \eta\right)}.$$

Proof. By the ε-sample condition we have

$$\|p - x\| \leq \varepsilon f(x)$$

since p is the closest sample point to x. The 1-Lipschitz continuity of the local feature size, see [1], implies that $f(p) \le f(x)/(1-\varepsilon)$. Putting both inequalities together proves claim (1).

In [1] it is shown that for any point $y \in V_p$ with $\|y - p\| > \mu f(p)$ the angle between the vector $y - p$ and the normal of S at p is upper bounded by

$$\arcsin(\eta/\mu) + \arcsin\eta.$$

Since $p^* \in V_p$ and $\|p^* - p\| > f(p)$ we have that the angle between the vector $p^* - p$ and the normal of S at p is upper bounded by $2\arcsin\eta$ and thus the angle between the vector $x - p$ and the normal of S at p is lower bounded by $\frac{\pi}{2} - 2\arcsin\eta$. Comparing the latter bound to $\arcsin(\eta/\mu) + \arcsin\eta$ and solving for μ gives

$$\mu = \frac{\eta}{\sin\left(\frac{\pi}{2} - 3\arcsin\eta\right)},$$

which proves claim (2).

The idea behind the next lemma is that the Voronoï cells of the sample points are long and thin and directed almost along the normals at the sample points. Therefore, edges that are almost tangential to the surface will appear early in the conformal alpha shape. We say that $p, q \in P$ are neighbors in a (conformal) alpha shape, if pq is a Delaunay edge that is contained in the alpha shape.

Lemma 7. *Let P be an ε-sample of a smooth surface S. The neighbors of $p \in P$ in a conformal alpha shape for small values of $\hat\alpha$ are at distance at most*

$$\left(\frac{1+\hat\alpha}{1-\hat\alpha}\right)\left(\frac{2\eta}{\sin\left(\frac{\pi}{2} - 3\arcsin\eta\right)}\right) f(p).$$

Proof. Let l be the vector $p^* - p$ as in Fig. 3 to the left.

We first want to bound the width of the smallest cylinder with axis l that contains the intersection of the Voronoï cell V_p of p with the ball of radius α_p centered at p. Let x be any point in the intersection of the boundary of V_p and the hyperplane containing p and orthogonal to l. Any hyperplane H supporting V_p at x must have p and p^* on the same side. In the limiting case, p^* is contained in H and so we consider this case. Then H contains a line l' through p^* and x. Let β be the acute angle made by l and l' at p^*, shown in Fig. 3 to the left. By Lemma 6,

$$\tan\beta = \frac{\|x-p\|}{\|p-p^*\|} \le \frac{\eta f(p)}{\alpha_p^+ \sin\left(\frac{\pi}{2} - 3\arcsin\eta\right)}.$$

The line l' intersects the boundary of the ball of radius $\alpha_p(\hat\alpha)$ centered at p in at most two points, as shown in Fig. 3 to the right. Let y be the intersection point furthest from p^*. Since we have chosen p^* and H to be the limiting case, the distance of y to l is an upper bound for the

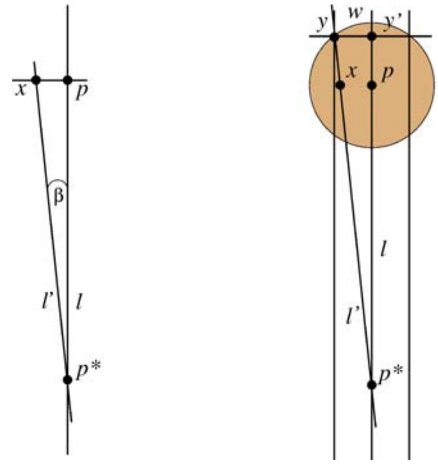

Fig. 3. Bounding $\tan\beta$ and the width w of the cylinder

width w of the cylinder we are looking for. Let y' be the projection of y onto l. Then,

$$\begin{aligned} w &\le \|y' - p^*\| \tan\beta \\ &= (\|p - p^*\| + \|y' - p\|)\tan\beta \\ &\le (\alpha_p^+ + \alpha_p(\hat\alpha))\tan\beta. \end{aligned}$$

Now let F be the affine hull of a Voronoï facet in V_p that is intersected by $C_p^{\hat\alpha}$. Again, p^* must be on the same side of F as p. The line l intersects F in a unique point. Let γ be the minimum angle between l and F at this intersection point, as shown in Fig. 4 to the right.

Then, we have

$$\tan\gamma \le \frac{w}{\|p - p^*\| - \alpha_p(\hat\alpha)} = \frac{w}{\alpha_p^+ - \alpha_p(\hat\alpha)}.$$

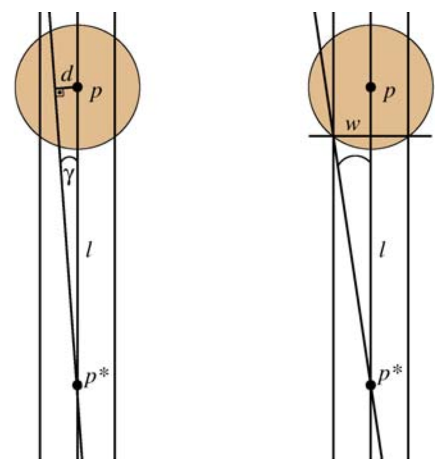

Fig. 4. Bounding $\tan\gamma$ and the distance d to a neighbor in the conformal alpha shape

The length d of the Delaunay edge dual to the Voronoï facet corresponding to F may be bounded by:

$$\begin{aligned} d &\le 2\|p-p^*\|\sin\gamma \\ &= 2\alpha_p^+\sin\gamma \\ &\le 2\alpha_p^+\tan\gamma \\ &\le \frac{2w\alpha_p^+}{\alpha_p^+-\alpha_p(\hat\alpha)} \\ &= \left(\frac{\alpha_p^+ + \alpha_p(\hat\alpha)}{\alpha_p^+ - \alpha_p(\hat\alpha)}\right) 2\|p-p^*\|\tan\beta \\ &\le \left(\frac{\alpha_p^+ + \alpha_p(\hat\alpha)}{\alpha_p^+ - \alpha_p(\hat\alpha)}\right)\left(\frac{2\eta}{\sin\left(\frac{\pi}{2}-3\arcsin\eta\right)}\right) f(p). \end{aligned}$$

This implies that all neighbors of p in a conformal alpha shape are at distance at most

$$\left(\frac{\alpha_p^+ + \alpha_p^+\hat\alpha}{\alpha_p^+ - \alpha_p^+\hat\alpha}\right)\left(\frac{2\eta}{\sin\left(\frac{\pi}{2}-3\arcsin\eta\right)}\right) f(p) = \left(\frac{1+\hat\alpha}{1-\hat\alpha}\right)\left(\frac{2\eta}{\sin\left(\frac{\pi}{2}-3\arcsin\eta\right)}\right) f(p).$$

This completes the proof.

Basically, Lemma 7 states that the conformal alpha shape is contained in a thickening of the surface S where the thickening factor with respect to the feature size depends on $\hat\alpha$ and η via

$$\left(\frac{1+\hat\alpha}{1-\hat\alpha}\right)\left(\frac{2\eta}{\sin\left(\frac{\pi}{2}-3\arcsin\eta\right)}\right).$$

Note that the thickening factor has two terms: a first part that only depends on the scale parameter $\hat\alpha$, and a second part that only depends on the sampling density ε. If $\hat\alpha = \eta$ and $\varepsilon < 0.1$, then $\eta < 0.112$ and this factor is less than 1. That is, the conformal alpha shape of an ε-sample with $\varepsilon < 0.1$ does not contain any point from the medial axis of the surface. This is true regardless of what the surface is, provided it is smooth. This contrasts with ordinary alpha shapes where for any $\varepsilon > 0$, we can give a surface such that the alpha shape contains a point of the medial axis.

Lemma 7 provides also further insight regarding the two permutations of the α-critical simplices according to the α and $\hat\alpha$ values, respectively. Suppose P is an ε-sample of a smooth surface S with $\varepsilon < 0.1$. Recently, it was shown that the intersection points of an α-critical simplex with its dual Voronoï cell is either very close to the surface S or very close to the medial axis $M(S)$, see [4]. Therefore, we can classify an α-critical simplex as either *surface-* or *medial-axis-critical*. By Lemma 7, we know that in the $\hat\alpha$-permutation of α-critical simplices, the surface-critical ones all appear before the medial-axis-critical. Therefore, conformal alpha shapes incorporate a local filtering that will allow surface reconstruction based on critical simplices.

The Crust and Cocone algorithms for surface reconstruction begin by filtering a set of *candidate triangles* from the Delaunay triangulation. An edge is *sharp*, if it has either a single incident triangle, or if any two consecutive triangles incident to it form an angle more than $3\pi/2$. In the second step, the algorithms remove all triangles incident on sharp edges. Finally, the algorithms compute a reconstruction by "walking" on either the inside or outside of the remaining set of candidate triangles. The resulting surface is homeomorphic to the original surface S, if P is a sufficiently dense ε-sample. The homeomorphism proof needs two properties of the set of candidate triangles. First, it has to contain all triangles of the restricted Delaunay triangulation $D_S(P)$. Second, all edges and triangles need to have a small circumradius compared to the feature size at their vertices.

We now show that a conformal alpha shape for a suitable value of $\hat\alpha$ may be used as the source of the candidate triangles, still giving us the topological guarantees after pruning and walking. Suppose we are given an ε-sample P of a smooth closed surface S with $\varepsilon < 0.1$. To show the homeomorphism property, we need to satisfy the two requirements discussed above. By Lemma 5, we know that the conformal alpha shape for $\hat\alpha = \eta = \varepsilon/(1-\varepsilon)$ contains the restricted Delaunay triangulation $D_S(P)$. It remains to show that all triangles in this conformal alpha shape have a small circumradius.

Lemma 8. *Let P be an ε-sample of a smooth surface S. All edges and triangles incident to $p \in P$ in a conformal alpha shape for $\hat\alpha < 1$ have circumradius at most*

$$\left(\frac{1+\hat\alpha}{1-\hat\alpha}\right)\left(\frac{\eta}{\sin\left(\frac{\pi}{2}-3\arcsin\eta\right)}\right) f(p).$$

Proof. For edges the statement is implied by Lemma 7. The circumradius of a Delaunay triangle is the distance d of any of its vertices to the line through its dual Voronoï edge. For a vertex p of a Delaunay triangle contained in the conformal alpha shape twice this distance can be bounded exactly same way as in the proof Lemma 7, where we bounded the length of the longest Delaunay edge incident to p and contained in the conformal alpha shape.

Therefore, we may compute a homeomorphic reconstruction of S from the conformal alpha shape of P with $\hat\alpha = \eta$.

4.3 Experimental results

We implemented the conformal alpha shape filtration using the C++ library CGAL. Fig. 5 illustrates the fundamental difference between α-shapes and conformal α-shapes. The point set shown in (a) contains a scaled version of a subset of itself. The globally uniform scale parameter of α-shapes, shown in (b) and (c) for two different α values, cannot recover the structure of the underlying manifold for any setting of α. Instead, a globally uniform and hence very dense sampling would be required, as shown in (d). In contrast, conformal α shapes can correctly reconstruct the correct curve (e) since the dual set of balls conforms to the local geometry of the point cloud. A 3D example is shown in bottom row of Fig. 5, where (f) shows the input point set, (g) the α-complex, and (h) the conformal α complex.

Fig. 6 shows a more difficult example. This data set is the result of curvature-adaptive surface simplification and is clearly not an ε-sampling with $\varepsilon < 0.1$. Thus both uniform and conformal α shapes fail to reconstruct the surface. Since the data set is highly non-uniform, α shapes perform poorly as expected. No single value of α provides a suitable complex for surface reconstruction. Conformal α-shapes behave more gracefully and provide a much better input for surface filtering as used in the final stage of the *Crust* and *Cocone* algorithms. Note that the latter algorithms would also fail on this data set. Both algorithms would provide a candidate triangle set similar to the one obtained for $\hat{\alpha} = 2.0$. Obviously, some regions of the shape are not captured adequately by the candidate triangles. For example, the mesh-based simplification algorithm created very few samples on the side of the nose, since this is a relatively flat region in the shape. However, the local feature size is very small, as the opposing parts of the nose come close together. As a result, the local conformal alpha ball is too small to introduce the required simplices, resulting in holes.

Although neither ordinary nor conformal alpha shapes succeed to reconstruct the surface it is still instructive to see the behavior of the complexes. In the α-filtration, triangles at more densely sampled features like the ears appear much earlier than triangles in other regions. For larger alpha values details at the ear get lost since already too many many triangles have appeared there, but at the same time sparsely sampled features like the back of the head have not been covered by triangles at all. This is in contrast to the $\hat{\alpha}$-filtration where for all values of $\hat{\alpha}$ all features of the shape are covered almost uniformly with triangles (of varying size) independent of how densely the features are sampled. For example the ears are not covered by large Delaunay triangles even for $\hat{\alpha} = 2.0$ whereas they small details of the ears are no longer visible already for $\alpha = 1.0$.

5 Conclusion

In this paper, we discuss conformal alpha shapes, a variation of the method of alpha shapes, that utilizes a local

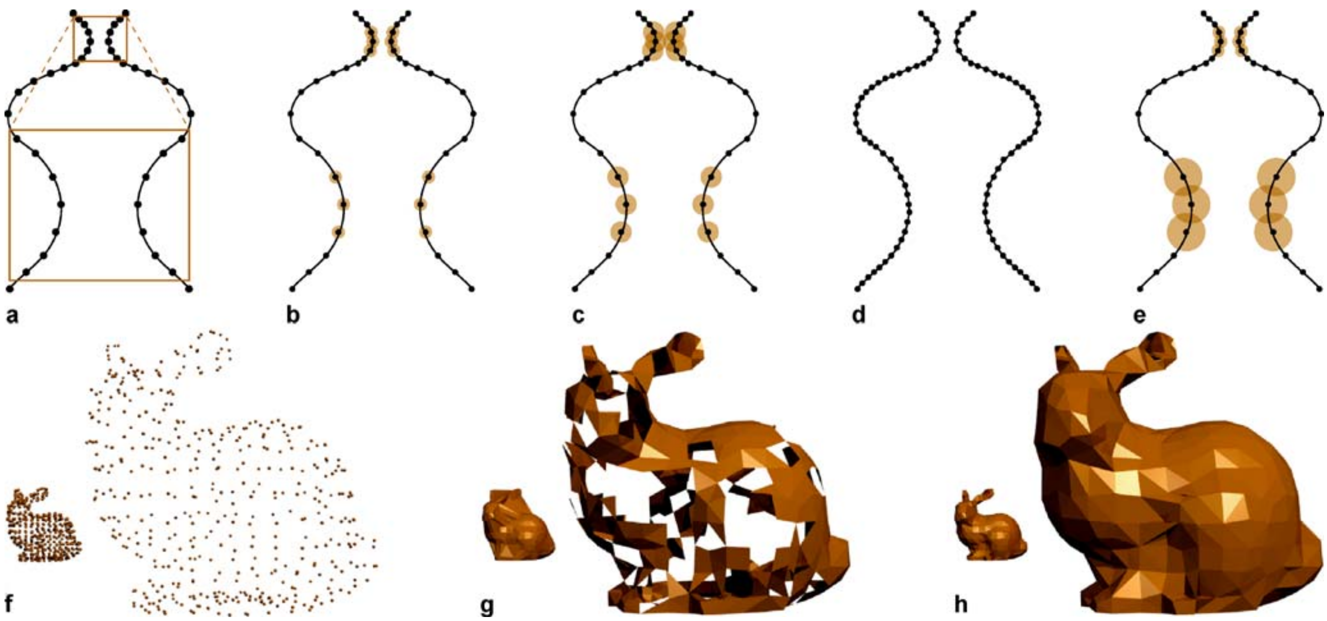

Fig. 5. Adapting the growth of the balls at the sample points as it is done for conformal α-shapes illustrates the superiority of conformal α-shapes (e) over uniform α-shapes (b,c) for curve and surface reconstruction from non-uniform samples (a). Uniform α-shapes would need uniform sampling as in (d). In (f) two scaled versions of a uniform sub-samples of the Stanford Bunny are shown in one scene to illustrate non-uniform sampling on a global scale. An α-shape for this sample is shown in (g) and a conformal α-shape is shown in (h)

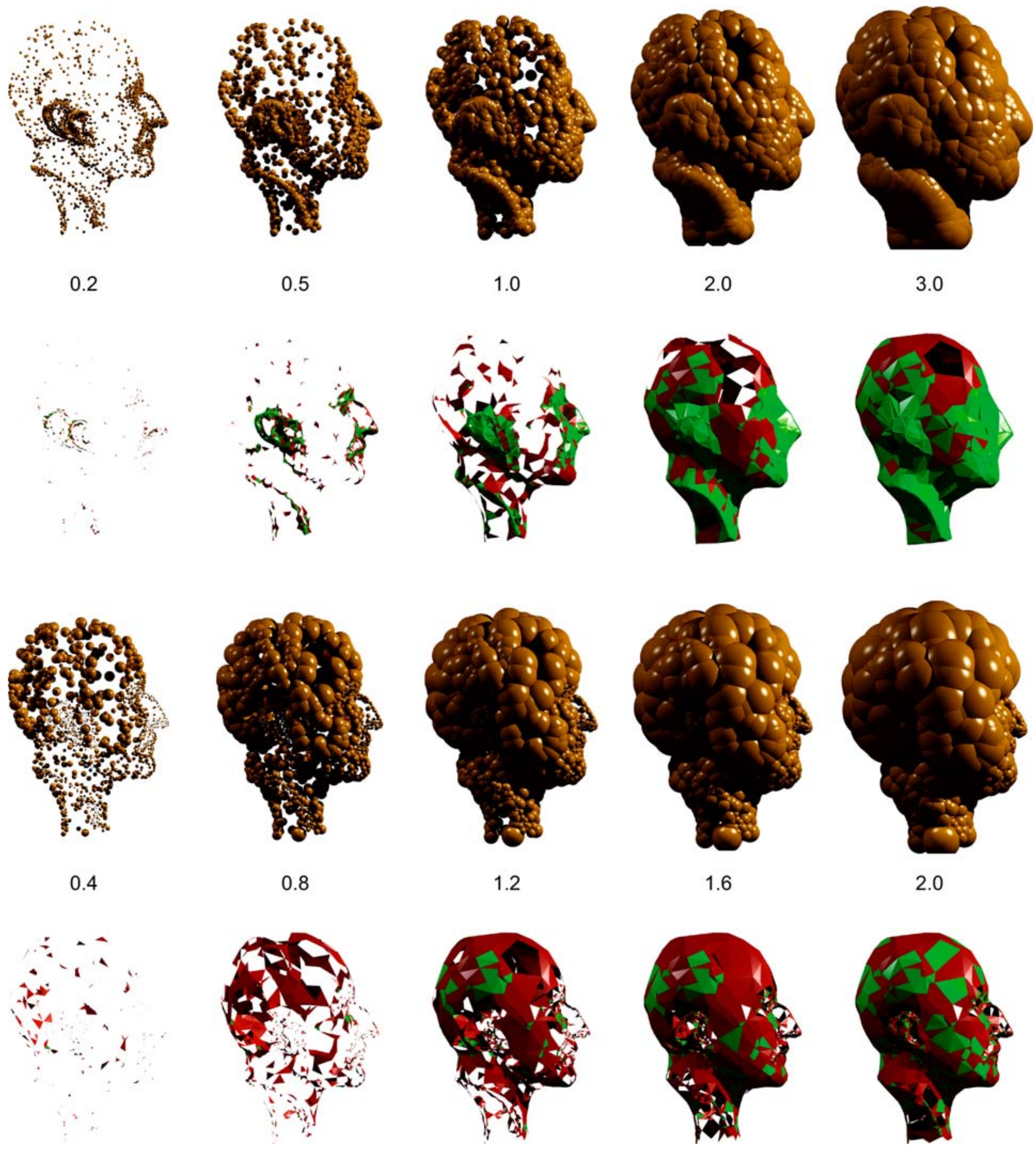

Fig. 6. Alpha shapes (upper half) vs. conformal alpha shapes (lower half). The top row shows the α- resp. $\hat{\alpha}$ balls and corresponding relative values of α and $\hat{\alpha}$. The bottom row shows the corresponding complex, where red color denotes singular 2-simplices and green shows faces of 3-simplices. Vertices and edges have been omitted for visual clarity

scale parameter $\hat{\alpha}$ that is invariant to scaling and Euclidean transformations. The local parameter reorders the simplices of the alpha shapes filtration into a new filtration. We show that this filtration has complexes that contain the restricted Delaunay simplices. As such, conformal alpha shapes can be utilized for provable surface reconstruction algorithms that compute candidate sets by filtering. Within the $\hat{\alpha}$-filtration, the critical simplices of the alpha shapes filtration remain critical. Moreover, the new ordering separates the critical simplices that are near the surface from those near the medial axis. Therefore, conformal alpha shapes may also be used by the second type of surface reconstruction algorithms that examine critical simplices. Conformal alpha shapes shed new light on the relationship between the two main approaches in Delaunay-based surface reconstruction algorithms.

Acknowledgement We thank Stefan Feistenauer for help with the implementation.

References

1. Amenta, N., Bern, M.: Surface reconstruction by Voronoi filtering. Discrete Comput. Geom. **22**, 481–504 (1999)
2. Amenta, N., Choi, S., Dey, T.K., Leekha, N.: A simple algorithm for homeomorphic surface reconstruction. In: 16th Annual ACM Symposium on Computational Geometry, pp. 213–222 (2000)
3. Cazals, F., Giesen, J., Pauly, M., Zomorodian, A.: Conformal alpha shapes. In: 2nd Symposium on Point Based Graphics, pp. 55–61 (2005)
4. Dey, T.K., Giesen, J., Ramos, E.A., Sadri, B.: Critical points of the distance to an epsilon-sampling on a surface and flow based surface reconstruction. In: 21st Annual ACM Symposium on Computational Geometry, pp. 218–227 (2005)
5. Edelsbrunner, H.: The union of balls and its dual shape. In: 9th Annual Symposium on Computational Geometry, pp. 218–231 (1993)
6. Edelsbrunner, H.: Geometry and Topology for Mesh Generation. Cambridge University Press, New York, NY (2001)
7. Edelsbrunner, H.: Surface reconstruction by wrapping finite point sets in space. Discrete Comput. Geom. **32**, 231–244 (2004)
8. Edelsbrunner, H., Facello, M.A., Liang, J.: On the definition and the construction of pockets in macromolecules. Discrete Appl. Math. **88**, 83–102 (1998)
9. Edelsbrunner, H., Kirkpatrick, D.G., Seidel, R.: On the shape of a set of points in the plane. IEEE Trans. Inform. Theory **IT–29**, 551–559 (1983)
10. Edelsbrunner, H., Mücke, E.P.: Three-dimensional alpha shapes. ACM Trans. Graphics **13**, 43–72 (1994)
11. Giesen, J., John, M.: The flow complex: A data structure for geometric modeling. In: 14th Annual ACM-SIAM Symposium on Discrete Algorithms, pp. 285–294 (2003)

FREDERIC CAZALS is research scientist in the Geometrica project at INRIA Sophia-Antipolis, France. He holds an engineering degree in Biological Sciences from the Institut National Agronomique Paris-Grignon, Paris, France, and a PhD in Computer Science from the University of Paris VII, Paris, France. His research interests include Surface Reconstruction and Shape Learning, Applied Differential Geometry, Computational Topology, and Computational Structural Biology.

JOACHIM GIESEN is a senior researcher in the "Theory of Combinatorial Algorithms" group in the computer science department at ETH Zurich. He received his Ph.D. from ETH Zurich in 2000 and afterwards joined Tamal K. Dey at the Ohio State University for a postdoc. His research interests are centered around algorithms and data structures with a focus on geometric algorithms.

MARK PAULY is an assistant professor at the computer science department of ETH Zurich, Switzerland, since April 2005. From August 2003 to March 2005 he was a postdoctoral scholar at Stanford University, where he also held a position as visiting assistant professor during the summer of 2005. He received his Ph.D. degree (with distinction) in 2003 from ETH Zurich and his M.S. degree (with honors) in computer science in 1999 from the Technical University of Kaiserslautern, Germany. His research interests include geometry processing, multi-scale shape modeling and analysis, physics-based animation, and computational geometry.

AFRA ZOMORODIAN is a Post-Doctoral Fellow in the Department of Computer Science at Stanford University. He received his B.S. from Stanford University in 1996 and his Ph.D. from University of Illinois at Urbana-Champaign in 2001, both in computer science. His research interests include computational topology and geometry.